

Novel Reddish-Orange-Emitting $\text{BaLa}_2\text{Si}_2\text{S}_8:\text{Eu}^{2+}$ Thiosilicate Phosphor for LED Lighting

Szu-Ping Lee,[†] Ting-Shan Chan,[‡] and Teng-Ming Chen^{*,†}

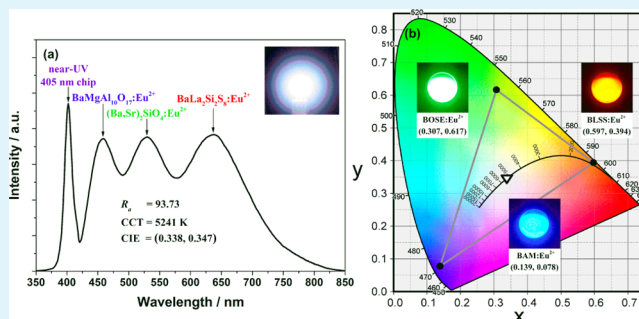
[†]Phosphors Research Laboratory, Department of Applied Chemistry and Institute of Molecular Science, National Chiao Tung University, Hsinchu 30010, Taiwan

[‡]National Synchrotron Radiation Research Center, Hsinchu 30076, Taiwan

S Supporting Information

ABSTRACT: A novel reddish-orange-emitting $\text{BaLa}_2\text{Si}_2\text{S}_8:\text{Eu}^{2+}$ thiosilicate was prepared in a sealed fused silica ampule and its crystal structure was refined using Rietveld methods. The $\text{BaLa}_2\text{Si}_2\text{S}_8:\text{Eu}^{2+}$ phosphor is excitable over a broad range from UV to blue (350–450 nm) and generated a reddish-orange broadband emission peaking at 645 nm with a quantum efficiency of ~24%. The thermal luminescence quenching of $\text{BaLa}_2\text{Si}_2\text{S}_8:\text{Eu}^{2+}$ was investigated over the range 25 to 150 °C. This phosphor was utilized to incorporate with two commercially available phosphors, blue $\text{BaMgAl}_{10}\text{O}_{17}:\text{Eu}^{2+}$ and green $(\text{Ba,Sr})_2\text{SiO}_4:\text{Eu}^{2+}$, and a near-UV LED chip (405 nm), a white light with R_a of ~94 was obtained.

KEYWORDS: photoluminescence, thiosilicate phosphor, LED lighting



In recent years, new red-emitting phosphors for displays and lighting have attracted much attention, because red light is essential in generating high color rendering index (CRI) and achieving lower correlated color temperature (CCT) warm white light for general lighting applications.^{1–4} In the generation of a broad red emission with good color purity, Eu^{2+} and Mn^{2+} have been widely studied.^{5–8} The luminescence of Eu^{2+} -activated phosphors could be excited over a broad range from the ultraviolet (UV) to near-ultraviolet (near-UV) regions and could be tuned from UV to red spectral regions. The intense broadband excitation and emission were attributed to the dipole-allowed 4f–5d electronic transitions of Eu^{2+} ions.⁹ On the other hand, phosphor materials including inorganic silicate compounds have been studied for use in various light sources and displays. Up to now, silicate, silicon nitride, silicon oxynitride, and thiosilicate materials have been reported.^{10–16} Particularly, thiosilicate materials exhibit the advantage that a relatively low synthetic temperature and various luminescence wavelengths have been reported.^{15–21} The emission of thiosilicate hosts doped with Ce^{3+} and Eu^{2+} covers the entire range from blue ($\text{Ba}_2\text{SiS}_4:\text{Ce}^{3+}$), green ($\text{Ca}_2\text{SiS}_4:\text{Ce}^{3+}$), yellow (Eu_2SiS_4), to red ($\text{Ca}_2\text{SiS}_4:\text{Eu}^{2+}$).^{16–18,21} The thermal quenching is limited for thiosilicate materials, for examples, $\text{Ca}_2\text{SiS}_4:\text{Eu}^{2+}$ retains 50% emission intensity at 200 °C,¹⁹ and $\text{Ba}_2\text{SiS}_4:\text{Ce}^{3+}$ keeps 80% emission intensity at 150 °C compared to the room-temperature case.¹⁷ It appears that thiosilicate materials can be a potential candidate for white LEDs.

In our previous work, a novel cyan-emitting Ce^{3+} -activated $\text{BaLa}_2\text{Si}_2\text{S}_8$ thiosilicate phosphor has been studied.²² In this research, we concentrate on the luminescence properties of

$\text{BaLa}_2\text{Si}_2\text{S}_8:\text{Eu}^{2+}$ thiosilicate phosphor and explored its potential to serve as a new phosphor-conversion material for solid-state lighting. Polycrystalline powder samples of $(\text{Ba}_{1-x}\text{Eu}_x)\text{La}_2\text{Si}_2\text{S}_8$ ($0.005 \leq x \leq 0.05$) was prepared by employing a solid-state reaction in a sealed fused silica ampule. Detailed experimental methods are provided in the Supporting Information.

The Rietveld analysis was accomplished to verify the purity of the phase and to acquire the detailed crystal structure parameters of $(\text{Ba}_{0.98}\text{Eu}_{0.02})\text{La}_2\text{Si}_2\text{S}_8$. The single-crystal structure data of $\text{La}_2\text{PbSi}_2\text{S}_8$ ²⁵ (ICSD No. 260733) were used as reference for a reliable approximation of the real crystal structure. There was no charge compensation issue for both Eu^{2+} and Ba^{2+} ions were of the same ionic charges, and the ionic radii (the coordination is 8) of Eu^{2+} ($r_{\text{Eu}^{2+}} = 125$ pm) and Ba^{2+} ($r_{\text{Ba}^{2+}} = 142$ pm) ions were also similar.²⁷ According to the mentioned reason, Eu^{2+} ions were incorporated in the Ba^{2+} sites of $\text{BaLa}_2\text{Si}_2\text{S}_8$. Figure 1a shows the SXRDR patterns of as-synthesized polycrystalline $(\text{Ba}_{0.98}\text{Eu}_{0.02})\text{La}_2\text{Si}_2\text{S}_8$, and the results were refined by using the GSAS software.^{23,24} The final expected R -factor (R_{exp}) and the weighted profile R -factor (R_{wp}) converged to 9.76% and 6.62%, respectively, which revealed the nice quality of the refinement.²³ $\text{BaLa}_2\text{Si}_2\text{S}_8$ is isostructural with $\text{PbR}_2\text{Si}_2\text{S}_8$ ($R = \text{Y, La–Nd, Sm, Gd–Ho}$) crystallizing trigonally in space group $R\bar{3}c$,²⁶ in which a mixture of La and Ba atoms have one crystallographic position and randomly occupy at a single site (18e).

Received: August 21, 2014

Accepted: December 23, 2014

Published: December 23, 2014



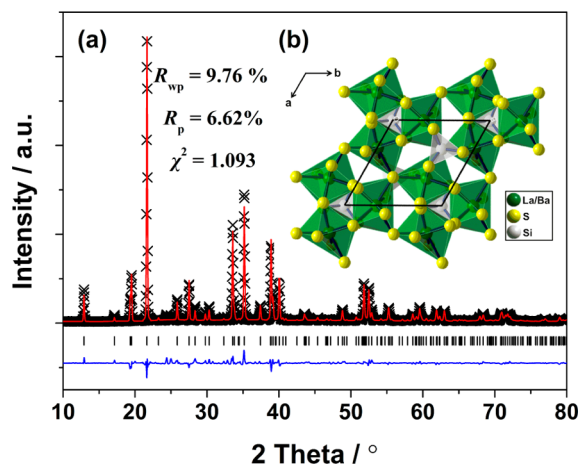


Figure 1. (a) Observed intensities (cross), calculated patterns (red line), Bragg positions (tick mark), and difference plot (blue line) SXRD profiles for Rietveld refinement results of $(\text{Ba}_{0.98}\text{Eu}_{0.02})\text{La}_2\text{Si}_2\text{S}_8$. (b) Unit-cell crystal structure representation of $(\text{Ba}_{0.98}\text{Eu}_{0.02})\text{La}_2\text{Si}_2\text{S}_8$, and the coordination environment around Ba/La/Si (Ba/La/Eu atom, green sphere; S atom, yellow atom; Si atom, white sphere).

Moreover, the chalcogen atoms and the Si atoms fully occupy at two sites (12c, 36f) and one site (12c), respectively. The crystallographic data and the selected atomic distances are summarized and available in the Supporting Information (Table S1 and S2). As shown in Figure 1b, the crystal lattice of $(\text{Ba}_{0.98}\text{Eu}_{0.02})\text{La}_2\text{Si}_2\text{S}_8$ is composed of $[\text{Si}_4]$ tetrahedral and bicapped trigonal prisms of $[(1/3\text{Ba} + 2/3\text{La})\text{S}_8]$, which are mutually connected by edges and corners.²⁶ The coordination polyhedron of Ba/La/Si consists of eight S and one Ba/La atoms situated at the center of the bicapped trigonal prism with a coordination number (CN) of 8.

The diffuse reflection spectra of as-synthesized polycrystalline $\text{BaLa}_2\text{Si}_2\text{S}_8$ and $(\text{Ba}_{0.98}\text{Eu}_{0.02})\text{La}_2\text{Si}_2\text{S}_8$ are presented in Figure 2. For the $\text{BaLa}_2\text{Si}_2\text{S}_8$ host, the diffuse reflection (DR) spectrum exhibits a high reflection in the wavelength range from 500 to 800 nm, and its reflection intensity decreased in the wavelength region from 250 to 500 nm. When 2 mol % Eu^{2+} is introduced into the $\text{BaLa}_2\text{Si}_2\text{S}_8$ host lattice, a notable reduction of reflectance ranging from 250 to 450 nm was

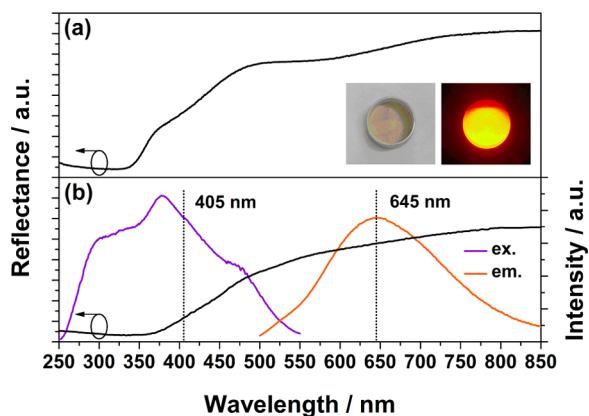


Figure 2. (a) Diffuse reflection (DR) spectrum of $\text{BaLa}_2\text{Si}_2\text{S}_8$ host. (b) DR spectrum, PLE spectrum ($\lambda_{\text{em}} = 645$ nm), and PL spectrum ($\lambda_{\text{ex}} = 405$ nm) of $(\text{Ba}_{0.98}\text{Eu}_{0.02})\text{La}_2\text{Si}_2\text{S}_8$. The insets show photographs of the prepared phosphor taken under normal light (left) and 365 nm UV light (right).

obtained, which means the absorption is enhanced. A typical excitation/emission spectra of $(\text{Ba}_{0.98}\text{Eu}_{0.02})\text{La}_2\text{Si}_2\text{S}_8$ is represented in Figure 2b. The excitation spectrum of $(\text{Ba}_{0.98}\text{Eu}_{0.02})\text{La}_2\text{Si}_2\text{S}_8$ shows broad absorption ranging from 250 to 500 nm, which matches well with the emission of near-UV LEDs, making $(\text{Ba}_{0.98}\text{Eu}_{0.02})\text{La}_2\text{Si}_2\text{S}_8$ interesting for solid-state lighting. In addition, the reddish-orange emission of the phosphor was assigned to the parity-allowed $4f^65d^1 \rightarrow 4f^7$ transition of Eu^{2+} ions.²⁸

The excitation and emission spectra of $(\text{Ba}_{1-x}\text{Eu}_x)\text{La}_2\text{Si}_2\text{S}_8$ ($0.005 \leq x \leq 0.05$) are shown in Figure 3. With an increase of

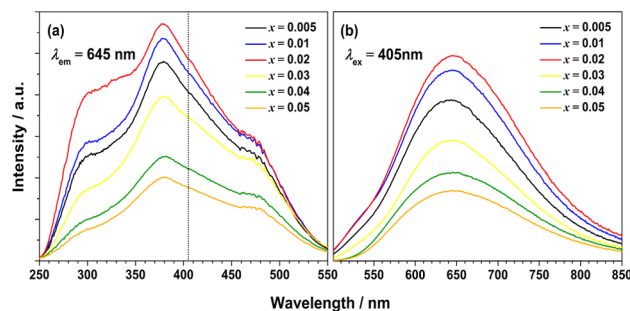


Figure 3. (a) Excitation spectra ($\lambda_{\text{em}} = 645$ nm) and (b) emission spectra ($\lambda_{\text{ex}} = 405$ nm) of $(\text{Ba}_{1-x}\text{Eu}_x)\text{La}_2\text{Si}_2\text{S}_8$ ($0.005 \leq x \leq 0.05$).

Eu^{2+} dopant concentration, the maximal emission wavelength shows a slight redshift; in contrast, the excitation spectra remain almost the same. Meanwhile, the optimal Eu^{2+} concentration is observed to be $x = 0.02$ (ca. 2 mol %) for the critical concentration (x_c), from which it can be utilized to discuss the concentration quenching caused by the energy transfer mechanisms, such as multipole–multipole interaction, exchange interaction and radiation reabsorption.²⁹ For the critical energy transfer distance (R_c), the following expression can be described.^{30,31}

$$R_c \approx 2 \left(\frac{3V}{4\pi x_c N} \right)^{1/3} \quad (1)$$

where V is the volume of the unit cell; x_c is the critical dopant concentration; N represents the number of total Eu^{2+} sites in the unit cell, respectively. In this case, $V = 1990.49 \text{ \AA}^3$, $x_c = 0.02$ (ca. 2 mol %), and $N = 6$. As a result, the R_c of Eu^{2+} was calculated to be 31.64 Å. Because the excitation and emission spectra do not overlap very well and generally the exchange interaction occurs in forbidden transition (the R_c is usually around 5 Å). According to the Dexter theory, the nonradiative concentration quenching between two nearest Eu^{2+} centers can be speculated to take place via electric multipolar interactions.³²

The decay curve of $(\text{Ba}_{0.98}\text{Eu}_{0.02})\text{La}_2\text{Si}_2\text{S}_8$ phosphor monitored at 645 nm under pulse laser excitation at 355 nm, as shown in Figure 4. As a result, it was found that $\text{Eu}^{2+} 4f^65d^1 \rightarrow 4f^7$ emission decays exponentially with lifetime $\sim 0.3656 \mu\text{s}$ and similar to that usually observed (0.4–1.2 μs).³³ The measured decay lifetime value can be described by using the first-order exponential equation.³⁴

$$I = I_0 \exp\left(\frac{-t}{\tau}\right) \quad (2)$$

where I represents the luminescence intensities at time t , I_0 is the luminescence intensities at time zero, and τ represents the decay lifetime.

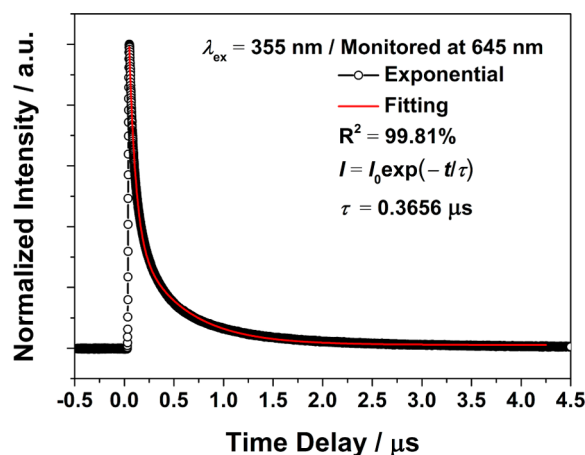


Figure 4. Decay curve of $(\text{Ba}_{0.98}\text{Eu}_{0.02})\text{La}_2\text{Si}_2\text{S}_8$ phosphor under 355 nm excitation and monitored at 645 nm.

The internal quantum efficiency (IQE) of $(\text{Ba}_{0.98}\text{Eu}_{0.02})\text{La}_2\text{Si}_2\text{S}_8$ was calculated to be $\sim 23.73\%$ under excitation at 405 nm. The obtained IQE can be further improved by optimization of preparation conditions. Furthermore, the temperature dependence of PL spectra for $(\text{Ba}_{0.98}\text{Eu}_{0.02})\text{La}_2\text{Si}_2\text{S}_8$ under excitation at 405 nm over the range 25 to 150 °C were investigated and illustrated in Figure 5. The PL

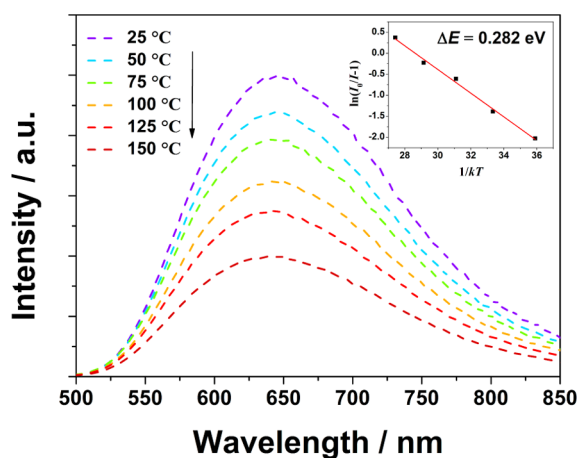


Figure 5. Temperature dependence of PL spectra for $(\text{Ba}_{0.98}\text{Eu}_{0.02})\text{La}_2\text{Si}_2\text{S}_8$ under excitation at 405 nm over the range 25–150 °C. The higher right inset represents the $\ln(I_0/I-1)$ versus $1/kT$ plot and the calculated activation energy (E_a) for the phosphor.

intensity of $(\text{Ba}_{0.98}\text{Eu}_{0.02})\text{La}_2\text{Si}_2\text{S}_8$ is diminished at high temperature compared to that discovered at room temperature for the reason that increasing temperature may increase the population of higher vibration levels, the density of phonons, and the probability of nonradiative transfer.³⁵ To verify the origin of the temperature dependence PL intensity $I(T)$, the activation energy (E_a) is related to the Arrhenius equation.³⁵

$$I(T) = \frac{I_0}{1 + A \exp\left(-\frac{E_a}{kT}\right)} \quad (3)$$

where I_0 and $I(T)$ are the integrated PL intensity at room temperature and testing temperature (25–150 °C), respectively, and k is the Boltzmann constant. The value of E_a for $(\text{Ba}_{0.98}\text{Eu}_{0.02})\text{La}_2\text{Si}_2\text{S}_8$ was estimated to be 0.2819 eV, as

indicated in the higher right inset in Figure 5. Recently, orange to red-emitting phosphors have been widely researched. For comparison, the luminescent properties of $\text{BaLa}_2\text{Si}_2\text{S}_8:\text{Eu}^{2+}$, $\text{Ca}_2\text{Si}_2\text{S}_4:\text{Eu}^{2+}$, and $\text{SrSi}_2\text{S}_4:\text{Eu}^{2+}$ are given in the Supporting Information (Table S3).^{18,19,36–38} It can be found that the full width at half-maximum (fwhm) of $\text{BaLa}_2\text{Si}_2\text{S}_8:\text{Eu}^{2+}$ is more than 170 nm ($58,823 \text{ cm}^{-1}$) broader than the others, which implies that a higher CRI value may be obtained when incorporated into pc-WLEDs. On the basis of the thermal luminescence quenching results, the stability of thiosilicate is comparable to that of binary sulfides.

To demonstrate the potential application of $(\text{Ba}_{1-x}\text{Eu}_x)\text{La}_2\text{Si}_2\text{S}_8$, the $(\text{Ba}_{0.98}\text{Eu}_{0.02})\text{La}_2\text{Si}_2\text{S}_8$ phosphor was incorporated into a pc-WLED device driven under forward bias current 350 mA with commercially available blue-emitting $\text{BaMgAl}_{10}\text{O}_{17}:\text{Eu}^{2+}$ phosphor, commercially available green-emitting $(\text{Ba,Sr})_2\text{SiO}_4:\text{Eu}^{2+}$ phosphor, and a 405 nm near-UV LED chip. The EL spectrum of this pc-WLED device is shown at Figure 6a, and the whole visible spectral region could be

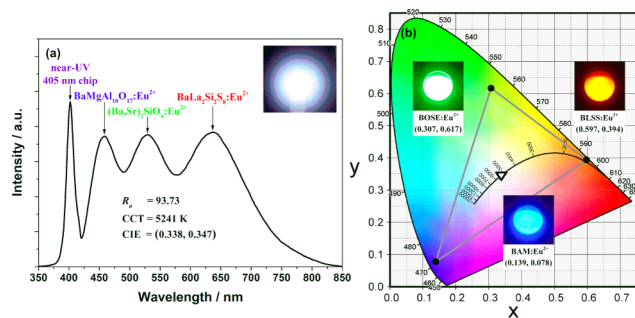


Figure 6. (a) EL spectrum of the device using 405 nm LED chip with blue-emitting $\text{BaMgAl}_{10}\text{O}_{17}:\text{Eu}^{2+}$ phosphor, green-emitting $(\text{Ba,Sr})_2\text{SiO}_4:\text{Eu}^{2+}$ phosphor, and red-emitting $\text{BaLa}_2\text{Si}_2\text{S}_8:\text{Eu}^{2+}$ phosphor. The inset shows the corresponding LED device photograph. (b) CIE chromaticity coordinates of the used phosphors and the fabricated LED are presented. The insets show the used phosphor photographs recorded under 365 nm excitation.

obtained when excited by the near-UV LED. The corresponding CCT, CRI, and CIE chromaticity coordinates (x, y) of this pc-WLED device was found to be 5241 K, 93.73, and (0.3382, 0.3475), respectively, as illustrated in Figure 6.

In summary, we have prepared and investigated the novel Eu^{2+} -doped thiosilicate phosphor with compositions of $(\text{Ba}_{1-x}\text{Eu}_x)\text{La}_2\text{Si}_2\text{S}_8$ ($0.005 \leq x \leq 0.05$) for the first time. The crystal structure, luminescence performance (i.e., PL/PLE intensity, chromaticity, IQE), decay lifetime, thermal luminescence property, and performance of white LED device were investigated and presented. The studies indicate that this novel reddish-orange phosphor is a potential candidate for white LED, especially for the generation of warm white light.

■ ASSOCIATED CONTENT

📄 Supporting Information

Details on the following topics: experimental methods, structural parameters, and the selected interatomic bond distances. This material is available free of charge via the Internet at <http://pubs.acs.org>.

■ AUTHOR INFORMATION

Corresponding Author

* E-mail: tmchen@mail.nctu.edu.tw.

Notes

The authors declare no competing financial interest.

ACKNOWLEDGMENTS

We appreciatively acknowledge the financial support by Ministry of Science and Technology of Taiwan under Contract NSC101-2113-M-009-021-MY3. We thank Dr. Dinesh Chandra Khara for luminescence decay lifetime measurement, and Dr. Chien-Hao Huang for assistance in pc-WLEDs fabrication.

REFERENCES

- (1) Ye, S.; Xiao, F.; Pan, Y. X.; Ma, Y. Y.; Zhang, Q. Y. Phosphors in Phosphor-Converted White Light-Emitting Diodes: Recent Advances in Material, Techniques and Properties. *Mater. Sci. Eng., R* **2010**, *71*, 1–34.
- (2) Xie, R. J.; Hirosaki, N. Review: Silicon-Based Oxynitrides and Nitride Phosphors for White LEDs. *Sci. Technol. Adv. Mater.* **2007**, *8*, 588–600.
- (3) Smet, P. F.; Moreels, I.; Hens, Z.; Poelman, D. Selecting Conversion Phosphors for White Light-Emitting Diodes. *J. Electrochem. Soc.* **2011**, *158*, R37–R54.
- (4) Smet, P. F.; Moreels, I.; Hens, Z.; Poelman, D. Luminescence in Sulfides: A Rich History and a Bright Future. *Materials* **2010**, *3*, 2834–2883.
- (5) Xie, R. J.; Hirosaki, N.; Suehiro, T.; Xu, F. F.; Mitomo, M. A Simple, Efficient Synthetic Route to $\text{Sr}_2\text{Si}_5\text{N}_8:\text{Eu}^{2+}$ -Based Red Phosphors for White Light-Emitting Diodes. *Chem. Mater.* **2006**, *18*, 5578–5583.
- (6) Piao, X. Q.; Machida, K. I.; Horikawa, T.; Hanzawa, H.; Shimomura, Y.; Kijima, N. Preparation of $\text{CaAlSiN}_3:\text{Eu}^{2+}$ Phosphors by the Self-Propagating High-Temperature Synthesis and Their Luminescent Properties. *Chem. Mater.* **2007**, *19*, 4592–4599.
- (7) Duan, C. J.; Delsing, A. C. A.; Hintzen, H. T. Photoluminescence Properties of Novel Red-Emitting Mn^{2+} -Activated MZnOS ($\text{M} = \text{Ca}, \text{Ba}$) Phosphor. *Chem. Mater.* **2009**, *21*, 1010–1016.
- (8) Jia, D. D.; Wang, X. J. Alkali Earth Sulfide Phosphors Doped with Eu^{2+} and Ce^{3+} for LEDs. *Opt. Mater.* **2007**, *30*, 375–379.
- (9) Huang, C. H.; Chen, T.-M. Novel Yellow-Emitting $\text{Sr}_8\text{MgLn}(\text{PO}_4)_7:\text{Eu}^{2+}$ ($\text{Ln} = \text{Y}, \text{La}$) Phosphors for Applications in White LEDs with Excellent Color Rendering Index. *Inorg. Chem.* **2011**, *50*, 5725–5730.
- (10) Kim, J. S.; Jeon, P. E.; Choi, J. C.; Park, H. L. Emission Color Variation of $\text{M}_2\text{SiO}_4:\text{Eu}^{2+}$ ($\text{M} = \text{Ba}, \text{Sr}, \text{Ca}$) Phosphors for Light-Emitting Diode. *Solid State Commun.* **2005**, *133*, 187–190.
- (11) Li, Y. Q.; Van Steen, J. E. J.; Van Kreveld, J. W. H.; Botty, G.; Delsing, A. C. A.; DiSalvo, F. J.; With, G.; Hintzen, H. T. Luminescence Properties of Red-Emitting $\text{M}_2\text{Si}_5\text{N}_8:\text{Eu}^{2+}$ ($\text{M} = \text{Ca}, \text{Sr}, \text{Ba}$) LED Conversion Phosphors. *J. Alloys Compd.* **2006**, *417*, 273–279.
- (12) Ruan, J.; Xie, R.-J.; Hirosaki, N.; Takeda, T. Nitrogen Gas Pressure Synthesis and Photoluminescent Properties of Orange-Red $\text{SrAlSi}_4\text{N}_7:\text{Eu}^{2+}$ Phosphors for White Light-Emitting Diodes. *J. Am. Ceram. Soc.* **2011**, *94*, 536–542.
- (13) Bachmann, V.; Ronda, C.; Oeckler, O.; Schnick, W.; Meijerink, A. Color Point Tuning for ($\text{Sr}, \text{Ca}, \text{Ba}$) $\text{Si}_2\text{O}_7:\text{Eu}^{2+}$ for White Light LEDs. *Chem. Mater.* **2009**, *21*, 316–325.
- (14) Xie, R. J.; Hirosaki, N.; Takeda, T.; Suehiro, T. On the Performance Enhancement of Nitride Phosphors as Spectral Conversion Materials in Solid State Lighting. *ECS J. Solid State Sci. Technol.* **2013**, *2*, R3031–R3040.
- (15) Smet, P. F.; Korthou, K.; Van Haecke, J. E.; Poelman, D. Using Rare Earth Doped Thiosilicate Phosphors in White Light Emitting LEDs: Towards Low Color Temperature and High Color Rendering. *Mater. Sci. Eng., B* **2008**, *146*, 264–268.
- (16) Parmentier, A. B.; Smet, P. F.; Poelman, D. Europium Doped Thiosilicate Phosphors of the Alkaline Earth Metals Mg, Ca, Sr and Ba: Structure and Luminescence. *Opt. Mater.* **2010**, *33*, 141–144.
- (17) Ohashi, T.; Ohmi, K. Improvement in Luminescent Characteristics by Al Codoping in $\text{Ba}_2\text{Si}_4\text{Ce}$ Blue Phosphor for White LEDs. *J. Light Vis. Environ.* **2008**, *32*, 139–142.
- (18) Smet, P. F.; Avci, N.; Loos, B.; Van Haecke, J. E.; Poelman, D. Structure and Photoluminescence of (Ca, Sr) $\text{Si}_4:\text{Eu}^{2+}$ Powders. *J. Phys.: Condens. Matter* **2007**, *19*, 246223.
- (19) Parmentier, A.; Smet, P. F.; Bertram, F.; Christen, J.; Poelman, D. Structure and Luminescence of (Ca, Sr) $\text{Si}_4:\text{Eu}^{2+}$ Phosphors. *J. Phys. D-Appl. Phys.* **2010**, *43*, 085401.
- (20) Nanai, Y.; Sakamoto, Y.; Okuno, T. Crystal Structure, Photoluminescence and Electroluminescence of (Ba, Eu) Si_2S_5 . *J. Phys. D* **2012**, *45*, 265102–265109.
- (21) Nishimura, M.; Nanai, Y.; Bohda, T.; Okuno, T. Yellow Photoluminescence of Europium Thiosilicate on Silicon Substrate. *Jpn. J. Appl. Phys.* **2009**, *48*, 072301–1–072301–4.
- (22) Lee, S. P.; Huang, C. H.; Chan, T. S.; Chen, T.-M. New Ce^{3+} -Activated Thiosilicate Phosphor for LED Lighting—Synthesis, Luminescence Studies, and Applications. *ACS Appl. Mater. Interfaces* **2014**, *6*, 7260–7267.
- (23) Larson, A. C.; Von Dreele, R. B. General Structure Analysis System (GSAS). *Los Alamos Nat. Lab. Rep. LAUR* **2004**, 86–748.
- (24) Toby, B. H. EXPGUI, A Graphical User Interface for GSAS. *J. Appl. Crystallogr.* **2001**, *34*, 210–213.
- (25) Gulay, L. D.; Daszkiewicz, M.; Ruda, I. P.; Marchuk, O. V. $\text{La}_2\text{Pb}(\text{Si}_3\text{S}_4)_2$. *Acta Crystallogr., Sect. C* **2010**, *C66*, i19–i21.
- (26) Shannon, R. D. Effective Ionic Radii and Systematic Studies of Interatomic Distances in Halides and Chalcogenides. *Acta Crystallogr., Sect. A: Cryst. Phys., Diffraction, Theor. Gen. Cryst.* **1976**, *32*, 751–767.
- (27) Daszkiewicz, M.; Marchuk, O. V.; Gulay, L. D.; Kaczorowski, D. Crystal Structures and Magnetic Properties of $\text{R}_2\text{PbSi}_2\text{S}_8$ ($\text{R} = \text{Y}, \text{Ce}, \text{Pr}, \text{Nd}, \text{Sm}, \text{Gd}, \text{Tb}, \text{Dy}, \text{Ho}$), $\text{R}_2\text{PbSi}_2\text{Se}_8$ ($\text{R} = \text{La}, \text{Ce}, \text{Pr}, \text{Nd}, \text{Sm}, \text{Gd}$) and $\text{R}_2\text{PbGe}_2\text{S}_8$ ($\text{R} = \text{Ce}, \text{Pr}$) Compounds. *J. Alloys Compd.* **2012**, *519*, 85–91.
- (28) Poort, S. H. M.; Van Kreveld, J. W. H.; Vink, R. A. P.; Blasse, G. Luminescence of Eu^{2+} in Host Lattices with Three Alkaline Earth Ions in a Row. *J. Solid State Chem.* **1996**, *122*, 432–435.
- (29) Wu, Y. C.; Wang, D. Y.; Chen, T.-M.; Lee, C. S.; Chen, K. J.; Kuo, H. C. A Novel Tunable Green- to Yellow-Emitting $\beta\text{-YFS}:\text{Ce}^{3+}$ Phosphor for Solid-State Lighting. *ACS Appl. Mater. Interfaces* **2011**, *3*, 3197–3199.
- (30) Blasse, G. Energy Transfer in Oxidic Phosphors. *Philips Res. Rep.* **1969**, *24*, 131–144.
- (31) Shang, M. M.; Li, G. G.; Kang, X. J.; Yang, D. M.; Geng, D. L.; Lin, J. Tunable Luminescence and Energy Transfer Properties of $\text{Sr}_3\text{AlO}_4\text{F}:\text{RE}^{3+}$ ($\text{RE} = \text{Tm}/\text{Tb}, \text{Eu}, \text{Ce}$) Phosphors. *ACS Appl. Mater. Interfaces* **2011**, *3*, 2738–2746.
- (32) Dexter, D. L. A Theory of Sensitized Luminescence in Solids. *J. Chem. Phys.* **1953**, *21*, 836–850.
- (33) Poort, S. H. M.; Meyerink, A.; Blasse, G. Lifetime Measurements in Eu^{2+} -Doped Host Lattices. *J. Phys. Chem. Solids* **1997**, *158*, 1451–1456.
- (34) Pang, R.; Li, C.; Shi, L.; Su, Q. A Novel Blue-Emitting Long-Lasting Propphosphate Phosphor $\text{Sr}_2\text{P}_2\text{O}_7:\text{Eu}^{2+}, \text{Y}^{3+}$. *J. Phys. Chem. Solids* **2009**, *70*, 303–306.
- (35) Xie, R. J.; Hirosaki, N.; Kimura, N.; Sakuma, K.; Mitomo, M. 2-Phosphor-Converted White Light-Emitting Diodes Using Oxynitride/Nitride Phosphors. *Appl. Phys. Lett.* **2007**, *90*, 191101–191103.
- (36) Smet, P. F.; Van Haecke, J. E.; Loncke, F.; Vrielinck, H.; Callens, F.; Poelman, D. Anomalous Photoluminescence in $\text{BaS}:\text{Eu}$. *Phys. Rev. B* **2006**, *74*, 035207–1–035207–9.
- (37) Kuo, T. W.; Liu, W. R.; Chen, T.-M. High Color Rendering White Light-Emitting Diodes Illuminator Using the Red-Emitting Eu^{2+} -Activated CaZnOS Phosphors Excited by Blue LED. *Opt. Express* **2010**, *18*, 8187–8192.
- (38) Ando, M.; Ono, Y. A. Temperature Effects in the Emission Characteristics of $\text{CaS}:\text{Eu}$ Thin-Film Electroluminescent Devices. *J. Cryst. Growth* **1992**, *117*, 969–974.

(39) Kim, K. B.; Kim, Y. I.; Chun, H. G.; Cho, T. Y.; Jung, J. S.; Kang, J. G. Structural and Optical Properties of $\text{BaMgAl}_{10}\text{O}_{17}:\text{Eu}^{2+}$ Phosphor. *Chem. Mater.* **2002**, *14*, 5045–5052.

(40) Shao, Q.; Lin, H.; Dong, Y.; Jiang, J. Temperature-Dependent Photoluminescence Properties of $(\text{Ba,Sr})_2\text{SiO}_4:\text{Eu}^{2+}$ Phosphors for White LEDs Applications. *J. Lumin.* **2014**, *151*, 165–169.